PRIMERJAVA ALGORITMOV ZA FILTRIRANJE ZA IZDELAVO DMR IZ LIDARSKIH PODATKOV: ŠTUDIJSKI PRIMER BERGAMA, TURČIJA

COMPARISON OF FILTERING ALGORITHMS USED FOR DTM PRODUCTION FROM AIRBORNE LIDAR DATA: A CASE STUDY IN BERGAMA, TURKEY

Baris Suleymanoglu, Metin Soycan

SI | EN

IZVLEČEK

Sistemi za aerolasersko skeniranje (lidar) spadajo med najpomembnejše tehnologije za izdelavo digitalnega modela reliefa (DMR). Oblak točk, ki jih s takšnimi rešitvami pridobimo, sestavljajo točke, ki se nanašajo na površje Zemlje (tla) in na ostale pojave v prostoru. Pri izdelavi DMR-ja jih je treba ločiti na točke tal in ostale točke. V ta namen so bili v preteklosti izdelani številni algoritmi za filtriranje oblaka točk. Namen študije je bil na štirih študijskih območjih z različno pokrovnostjo tal ipreizkusiti šest različnih algoritmov za filtriranje oblaka točk. Algoritmi, ki smo jih preizkusili, so bili prilagodljiva mreža neenakih trikotnikov ATIN (angl. adaptive triangulated irregular network), višinski prag z razširjenim oknom ETWE (angl. elevation threshold with an expand window), največji lokalni naklon MLS (angl. maximum local slope), progresivna morfologija PM (angl. progressive morphology), iterativno polinomsko prileganje IPF (angl. iterative polynomial fitting) ter klasifikacija ukrivljenosti MCC (angl. multiscale curvature classification). Dobljeni rezultati so bili dobri za vse uporabljene filtre pri gladkih površinah, več napak pa se je pojavilo na kompleksnih urbanih območjih in na razgibanem terenu z gosto vegetacijo. Algoritem IPF se je najbolje izkazal za prva tri študijska območja, za četrto območje se je najbolje izkazal algoritem ETEW.

ABSTRACT

A light detection and ranging (lidar) system is one of the most important technologies used for generating digital terrain models (DTMs). The point cloud data obtained by these systems consist of data gathered from ground and nonground features. To create a DTM with high resolution and accuracy, ground and nonground data must be separated. Numerous filtering algorithms have been developed for this purpose. The aim of this study was testing the filtering performance of six different filtering algorithms in four different test areas with different land cover were selected that had topographical features and characteristics. The algorithms were adaptive triangulated irregular network (ATIN), elevation threshold with an expand window (ETEW), maximum local slope (MLS), progressive morphology (PM), iterative polynomial fitting (IPF), and multiscale curvature classification (MCC) algorithms. In the results, all the filters performed well on a smooth surface and produced more errors in complex urban areas and rough terrain with dense vegetation. The IPF filtering algorithm generated the best results for the first three test areas (smooth landscape, urban areas and agricultural areas), while ETEW performed best in the fourth test area (steep areas with dense vegetation and infrastructure).

KLJUČNE BESEDE

KEY WORDS

Baris Suleymanoglu, Metin Soycan | PRIMERJAVA ALGORITMOV ZA FILTRIRANJE ZA IZDELAVO DMR IZ LIDARSKIH PODATKOV: ŠTUDIJSKI PRIMER BERGAMA, TURČIJA | COMPARISON OF FILTERING ALGORITHMS USED FOR DTM PRODUCTION FROM AIRBORNE LIDAR DATA: A CASE STUDY IN BERGAMA, TURKEY | 395-414 |

| 395 |

1 INTRODUCTION

As an active remote-sensing technology, light detection and ranging (lidar) systems use laser pulses for measuring the nonvertical distances between lidar sensors and ground surfaces (Wever and Lindenberger, 1999). Lidar systems are important measurement systems that have been increasing in popularity in recent decades; lidar can be integrated with different platforms (aircraft, helicopter, unmanned aerial vehicle), and the system consists of a laser scanner integrated with a global positioning system (GPS) and inertial navigation unit (INS) (Wehr and Lohr, 1999). Hence, high-density and high-accuracy three-dimensional (3D) data can be obtained with lidar systems (Habib et al., 2005). Over the past two decades, many studies have been performed on the processing and application of lidar data. Lidar point cloud data have become the main source of terrain-related applications, such as the generation of digital surface models (DSMs), digital terrain models (DTMs), 3D urban modeling, hydrological modeling, glacier monitoring, flood plain assessment, and the detection of electrical powerlines (e.g., Axelsson, 1999; Hodgson et al., 2005; Liu, 2008). Although lidar data can be used in a wide variety of applications, DTMs constitute a key element for their realization (Chen et al., 2017).

Lidar data capture fast and accurate 3D point data for large areas; moreover, they are unaffected by the presence of light and can penetrate vegetation and capture points beneath a forest canopy. Thus, they overcome the disadvantages of conventional measurement methods like field surveying and photogrammetry (Kraus and Pfeifer, 1998). Such data are becoming the primary tool for the production of DTMs. In this context, some countries or states are working to acquire national coverage of lidar data and DTMs (Pfeifer and Mandlburger, 2018). In fact, some countries have carried out nationwide data acquisition using lidar; the Netherlands did so for the second time in 2012 and decided to update these data regularly (Vosselman et al., 2015). Such developments illustrate that lidar data and DTMs are becoming standard products released from national geoportals (Krishnan et al., 2011).

Despite their advantages, lidar point cloud data include various ground and nonground objects, such as buildings, bridges, trees, cars, and the ground, that must be differentiated (Liu, 2008). The separation of ground and nonground points to generate highly accurate DTMs is called *filtering* (Briese, 2010). Numerous filtering algorithms have been developed for extracting ground (bare land) points from raw lidar data. However, each developed filtering algorithm has weaknesses and strengths, and its performance depends on the surface types (Sithole and Vosselman, 2004). To determine the strengths and weaknesses of the filtering algorithms, it is necessary to test them on diverse landscapes, and the results must be analyzed qualitatively and quantitatively.

According to Briese (2010) and Pfeifer and Mandlburger (2018), filtering algorithms can be divided into four different categories, which are as follows: morphological filtering, progressive densification, surface-based filtering, and segment-based filtering algorithms. Morphological filtering algorithms are based on the concept of mathematical morphology. The two basic operators used in this approach are erosion and dilation. With the consecutive use of these two operators, closing (erosion-dilation) and opening (dilation-erosion) operators are applied. Minimum and maximum objects can be determined in the structure element (Haralick and Shapiro, 1992; Briese, 2010). Vosselman (2000) developed a filtering algorithm based on a mathematical morphology that uses admissible height differences as a function of the Euclidean distance between points. A modified version of this filtering algorithm was

Baris Suleymanoglu, Metin Soycan | PRIMERJAVA ALGORITMOV ZA FILTRIRANJE ZA IZDELAVO DMR IZ LIDARSKIH PODATKOV: ŠTUDIJSKI PRIMER BERGAMA, TURČIJA | COMPARISON OF FILTERING ALGORITHMS USED FOR DTM PRODUCTION FROM AIRBORNE LIDAR DATA: A CASE STUDY IN BERGAMA, TURKEY |395-414|

| 396 |

developed and presented by different researchers (Sithole, 2001; Zaksek and Pfeifer, 2006). Sithole (2001) developed a local operator that can be changed based on the slope of the terrain, while Zaksek and Pfeifer (2006) introduced an inclined slope operator for eliminating the effect of terrain relief. To remove different-sized objects, Kilian et al. (1996) employed multiple structure elements (i.e., windows) and assigned weights to points depending on the window size. In the progressive morphological filter developed by Zhang et al. (2003), the size of the window was determined by the slope of the terrain. Several additional morphological filters have been developed by other authors (Susaki, 2012; Pingel et al., 2013; Li et al., 2014; Mongus et al., 2014).

Progressive densification represents another important filtering algorithm group. This type of filter works progressively with the help of a triangulated irregular network (TIN). Axelsson (2000) introduced a progressive densification filtering process with a different filtering strategy; it starts with a small subset of point cloud data and iteratively increases the point data. In this approach, the first data subset is generated with a simple block minimum filter (Briese, 2010). Then, for each iteration, a point is added to the TIN if it matches certain criteria. This process ends when no more points are added to the TIN surface or no more points are below the threshold. This filtering algorithm is also used in commercial software, such as Terrasolid (Chen et al., 2017). Sohn and Dowman (2002) applied progressive densification with an initial downward step to find points below the TIN surface, and they updated the model using these points. Thereafter, an upward step was conducted for determining the appropriate points according to the threshold value. Other progressive filters have been developed by Guan et al. (2014), Chen et al. (2016), and Zhang and Lin (2013).

Kraus and Pfeifer (1998) developed a surface-based filter using least-squares interpolation. This algorithm works iteratively. First, rough terrain is generated using all the data. Following this, an averaging surface is created between the ground and nonground points. Residuals are created according to their distance from the averaging surface, and weight is attached to the points according to their residual values. Points that have negative residual values are weighted more heavily and are considered ground points (Pfeifer et al., 2001). Elmqvist (2001) used an active shape model for representing the terrain surface. Starting from last-return points, Chen et al. (2012) separated lidar points into different elevation layers. The detection of ground points and refining of the output DTMs were carried out from the top to the bottom layer. Zhang et al. (2016) used a cloth simulation from computer science. The cloth shape was set by the functions of gravity, intersections, and inner forces of the cloth. Finally, based on the cloth particles, lidar points were filtered (Chen et al., 2017).

Unlike the approaches of previous filtering algorithms, segment-based filtering algorithms aim to classify neighbouring points by looking at the similarities between points instead of classifying them one by one. Sithole and Vosselman (2005) and Tóvári and Pfeifer (2005) developed and presented this approach, where the goal was overcoming the difficulties in filtering the single points.

In addition to these four methods, other filtering approaches have been developed and used. Wu et al. (2011) employed support vector machines, while Hu and Yuan (2016) used the deep convolutional neural network method to classify lidar point cloud data. Jahromi et al. (2011) employed artificial neural networks. Furthermore, Bartels and Wei (2010) developed a threshold-free algorithm for automating the filtering process to a high level, especially for reducing the dependence of the threshold value. In addition,

Baris Suleymanoglu, Metin Soycan | PRIMERJAVA ALGORITMOV ZA FILTRIRANJE ZA IZDELAVO DMR IZ LIDARSKIH PODATKOV: ŠTUDIJSKI PRIMER BERGAMA, TURČIJA | COMPARISON OF FILTERING ALGORITHMS USED FOR DTM PRODUCTION FROM AIRBORNE LIDAR DATA: A CASE STUDY IN BERGAMA, TURKEY |395-414|

| 397 |

in point cloud classification studies, full-waveform lidar data have been increasingly investigated due to providing extra features, such as the echo width of the object surfaces (Pfeifer and Mandlburger, 2018). Mallet et al. (2011) classified lidar data into ground, vegetation, and building points using differential laser cross-sections generated from full-waveform lidar data. Finally, Jutzi and Stilla (2005) performed urban land classification using the relationship between neighbouring waveforms.

As indicated above, many algorithms have been developed for filtering lidar point cloud data. Multiple studies comparing lidar filtering algorithms have been published, including those by Sithole and Vosselman (2004), Podobnikar and Vrečko (2012), Mongus et al. (2013), Julge et al. (2014), and Zhao et al. (2018). However, the performances of filtering algorithms are generally tested under specific topographic and environmental conditions. Therefore, there is still a need for further investigation of the effects of different classes of land use and land cover on filtering algorithms' performance (Silva et al., 2018).

Although many filtering algorithms have been proposed, there are still some difficulties with filtering lidar point cloud data. The performance results of the filtering algorithms vary under different terrain situations, and each algorithm has unique strengths and limitations in certain situations (Chen et al., 2017). Therefore, the aim of this study is investigating the effects of terrain and environmental factors on the performance of different filtering algorithms that are widely used today. In addition, the use of point cloud data obtained from lidar systems by private and public institutions is gradually increasing in our country. Hence, the results of this study can help decide which single or combination of filtering techniques are appropriate for use. Therefore, the performance of these filtering methods was examined in different test areas, which are the most common topographic surfaces in our country, such as surfaces mixed with different topographic objects (i.e., a small valley, open landscape, high and low vegetation), building-dominated urban areas, vegetated mountains, and agricultural land with crops and shrubs. Furthermore, the aim is determining the most suitable filtering algorithm for specific test areas and the appropriate parameter values for each filtering algorithm for each test area. To accomplish this, the filtering results are analyzed qualitatively and quantitatively in terms of reference data filtered manually via visual inspection. In the next section, the mathematical models and basic principles of these filtering methods are briefly explained. Finally, the results of the filtering are analyzed in detail, and the paper concludes with a brief summary.

2 FILTERING METHODS

The filtering algorithms used in this study are classified as morphological (maximum local slope [MLS], progressive morphology [PM]), progressive densification (adaptive triangulated irregular network [ATIN]), surface-based (iterative polynomial fitting [IPF]), and other filtering (elevation threshold with an expand window [ETEW], multiscale curvature classification [MCC]) algorithms among the classes determined by Briese (2010) and Pfeifer and Mandlburger (2018). Filtering is performed using the ALDPAT (ETEW, MLS, PM, IPF, ATIN) (Zhang and Cui, 2007) and MCC-Lidar (Evans and Hudak, 2007) software programs.

2.1 Elevation Threshold with an Expand Window (ETEW) Filter

This filtering algorithm starts with the division of the test area into square cells; all points except the minimum elevation are excluded. Cell sizes are increased iteratively, and filtering is performed by compar-

Baris Suleymanoglu, Metin Soycan | PRIMERJAVA ALGORITMOV ZA FILTRIRANJE ZA IZDELAVO DMR IZ LIDARSKIH PODATKOV: ŠTUDIJSKI PRIMER BERGAMA, TURČIJA | COMPARISON OF FILTERING ALGORITHMS USED FOR DTM PRODUCTION FROM AIRBORNE LIDAR DATA: A CASE STUDY IN BERGAMA, TURKEY | 395-414 |

| 398 |

ing the height differences between the threshold values. The filtering algorithm works iteratively until no more points are added to the ground. Formulas (1), (2), and (3) are adopted from Zhang and Whitman (2005) and Zhang and Cui (2007):

$$Z_{i,j} - Z_{i,min} > h_{i,T},$$ (1)

$$h_{i,T} = s*c_i,$$ (2)

$$c_i = 2*c_{i-1} \quad i = 2,3,...M.$$ (3)

Here, $Z_{i,j}$ represents the height of each point ($p_{i,j}$) in the cells; the minimum height in the cell is $Z_{i,min}$, and $h_{i,T}$ is the height threshold, which is calculated based on the maximum slope value (s) and cell size parameter (c_i). The cell size is doubled at each iteration (c_i). M specifies the total number of iterations.

2.2 Maximum Local Slope (MLS)

This filtering algorithm classifies ground data using the slope values between a lidar point and its neighbors. The MLS algorithm used in the ALDPAT software is comparable to Vosselman's (2000) filter. Lidar data $p_o(x_o, y_o, z_o)$ are classified as ground points when the maximum slope (s_0, max) between points is less than the threshold value (s):

$$s_{o,j} = \frac{z_o - z_j}{\sqrt{(x_o - x_j)^2 + (y_o - y_j)^2}},$$ (4)

if $s_{o,max} < s \longrightarrow p_o$ classified as ground data. (5)

2.3 Progressive Morphological (PM) Filter

A PM filter was developed by Zhang et al. (2003). The points with the minimum height in the cell are selected, and the approximate surface is created. Secondary surfaces are generated by applying an opening operation to the initial surface. The differences between the two surfaces are compared with the threshold value; points below the value are selected as ground points. The window size must be larger than the largest object in the workspace so that nonground objects can be filtered effectively. During filtering, the window size is increased iteratively, and ground points are selected according to the elevation threshold (Zhang and Cui, 2007). The threshold value $dh_{i,T}$ is calculated as follows:

$$\begin{aligned} &dh_o & &\text{if } w_i \leq 3, \\ &dh_{i,T} = s(w_i - w_{i-1})*c + dh_o & &\text{if } w_i > 3, \\ &dh_{max} & &\text{if } dh_{i,T} > dh_{max}. \end{aligned}$$ (6)

2.4 Iterative Polynomial Fitting (IPF) Filter

Unlike other algorithms, the IPF filtering algorithm iteratively selects the ground data from the original dataset. It starts with the selection of the points with the lowest height in the large moving window centred over each grid node. These represent the initial set of ground points. Then, the window size is reduced and new candidate points for the ground are selected. A candidate point is classified as a ground point if the elevation difference between the candidate and interpolated surface is less than a predefined threshold. This process continues until the window size is smaller than the grid spacing is (Zhang and Cui, 2007).

Baris Suleymanoglu, Metin Soycan | PRIMERJAVA ALGORITMOV ZA FILTRIRANJE ZA IZDELAVO DMR IZ LIDARSKIH PODATKOV: ŠTUDIJSKI PRIMER BERGAMA, TURČIJA | COMPARISON OF FILTERING ALGORITHMS USED FOR DTM PRODUCTION FROM AIRBORNE LIDAR DATA: A CASE STUDY IN BERGAMA, TURKEY | 395-414 |

| 399 |

2.5 Multiscale Curvature Classification (MCC)

The MCC filtering algorithm first constructs the surface using all the points with thin-plate spline interpolation; following this, the interpolation surface is smoothed using 3 x 3 kernel functions and the curvature tolerance is added to each cell. If the z value of a point is greater than the curvature threshold point, it is classified as a nonground point. This process is performed iteratively in the three-scale domain, and the threshold is recalculated at each step (Evans and Hudak, 2007).

2.6 Adaptive Triangulated Irregular Network (ATIN) Filter

In the ATIN filter, first, the test area is subdivided into user-defined small cells and the minimum elevation is selected. These local minimum points are considered ground points. Next, a rough TIN is generated based on seed points using the Delaunay triangulation algorithm. All the points except for seed points are examined in terms of their distance to the TIN surface and maximum of three angles between the triangle surface. If the distance and angle of a point are less than the predefined threshold, the point is added to the ground points. The TIN is created using these new points. This process iteratively continues until all points are classified as ground or nonground (Zhang and Cui, 2007).

3 MATERIALS AND METHODS

3.1 Examination and Comparison of the Filtering Methods in Different Test Areas

In this study, the performance of the abovementioned filtering algorithms in our test areas was investigated, and the most appropriate parameter values were determined for these areas. Filtering was carried out using specified parameter values, and a comprehensive statistical analysis was conducted for the results. Detailed information on the data and test area used in this study, the methodology used for data processing, and comparison and analysis of the results are explained in the sections below.

3.2 Test Areas and Data

The lidar data used in this study were collected by the General Directorate of Mapping in Bergama County, İzmir Province, Turkey. The flight was accomplished with an Optech Pegasus HA-500 on October 20–21, 2014 from a flying height of 1,200 m (Kayi et al., 2015). The parameters for the test flight were as follows:

- Flight height: 1,200 m;
- Field of view: ±35°;
- Scanning mechanism: oscillating mirror;
- Swath width: 580 m;
- Flying speed: 277.8 km/h; and
- Overlap: 25%.

The accuracy of the point cloud data obtained with the Optech Pegasus HA-500 system was tested with 51 control points. These were measured using a TUSAGA-Active RTK GNSS. Among these points, 26 were used as the control points for georeferencing the point cloud and 25 points used as checkpoints for calculating the vertical accuracy. The root mean square error (RMSE) of the point cloud data was 0.07 m for the vertical accuracy of the checkpoints (Kayi et al., 2015).

Baris Suleymanoglu, Metin Soycan | PRIMERJAVA ALGORITMOV ZA FILTRIRANJE ZA IZDELAVO DMR IZ LIDARSKIH PODATKOV: ŠTUDIJSKI PRIMER BERGAMA, TURČIJA | COMPARISON OF
FILTERING ALGORITHMS USED FOR DTM PRODUCTION FROM AIRBORNE LIDAR DATA: A CASE STUDY IN BERGAMA, TURKEY | 395-414 |

| 400 |

Table 1: Statistical values for the test areas.

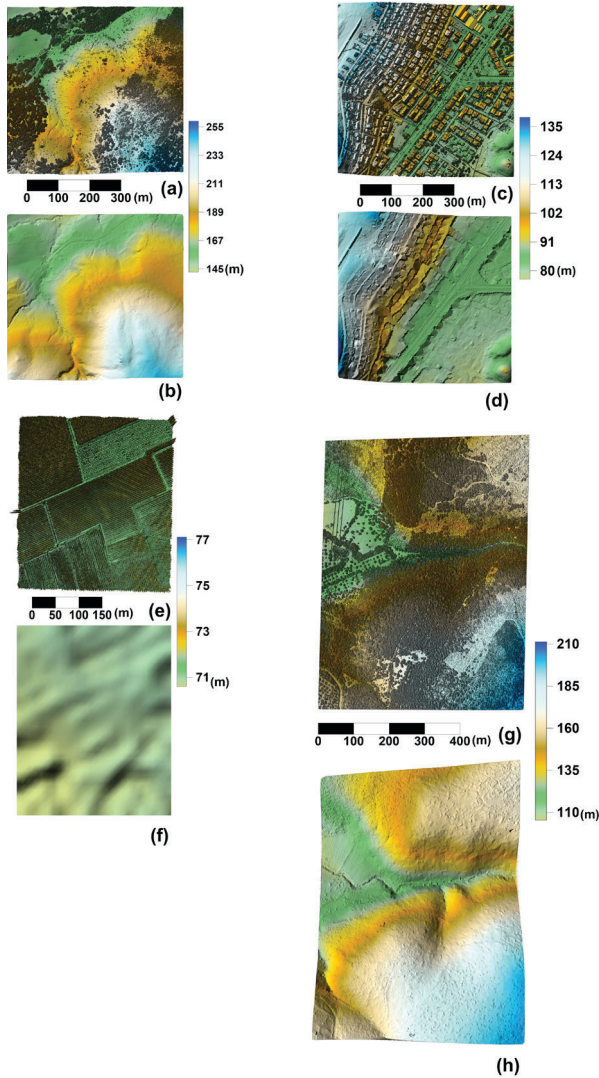| Parameters	First Test Area	Second Test Area	Third Test Area	Fourth Test Area
Area (km²)	0.36	0.36	0.13	0.44
Point Density (pt/m²)	24	17	14	17
Max. Height (m)	259.73	139.04	74.79	211.97
Min. Height (m)	141.25	76.83	70.55	105.34
Mean slope for raw data (deg)	45.30	33.25	6.86	50.25
Mean slope for reference data (deg)	11.85	7.8	1.45	15.09

Figure 1: Digital surface model of first (a), second (c), third (e) and fourth (g) test area , digital terrain model of first (b), second (d), third (f) and fourth (h) test area.

Baris Suleymanoglu, Metin Soycan | PRIMERJAVA ALGORITMOV ZA FILTRIRANJE ZA IZDELAVO DMR IZ LIDARSKIH PODATKOV: ŠTUDIJSKI PRIMER BERGAMA, TURČIJA | COMPARISON OF FILTERING ALGORITHMS USED FOR DTM PRODUCTION FROM AIRBORNE LIDAR DATA: A CASE STUDY IN BERGAMA, TURKEY | 395-414 |

| 401 |

Four test areas with different terrain characteristics and objects (roads, buildings, vegetation) were selected. The first test area (Figure 1a,b) consists of diverse terrain features, such as small valleys, open landscape, and rural roads. Trees of different types and sizes are also spread throughout the study area. The second test area (Figure 1c,d) was selected from low-relief urban spaces at the centre of Bergama County. It includes different-sized residential houses, large factory buildings, trees, highways, and open landscape. The third test area (Figure 1e,f) was selected from a relatively flat agricultural area consisting of crops and shrubs. The vegetation heights for the study area varied between 50 cm and 2 m, which can be classified as low vegetation in accordance with the American Society for Photogrammetry and Remote Sensing (ASPRS) LAS file format specifications (low vegetation: 0.5 m < height < 2 m; Khosravipour et al., 2014). The fourth test area (Figure 1g,h) consists of steep slope valleys covered with dense vegetation. In this study area, different-sized vegetation is located on the slopes. In addition, there is a riverbed, transmission towers, and areas covered with low and high trees. Detailed statistics on both test areas are listed in Table 1. The DSMs and DTMs of all the test areas are illustrated in Figure 1. The DTMs were generated from a rough filtering process for visualizing the terrain characteristics.

3.3 Processing of the Test Data and Comparative Methodology

Many parameters are influential in the practical use of the filtering models summarized in the previous section. The correct determination of these parameters directly affects the filtering results. Hence, the aim of this study was determining the most suitable filtering algorithm and appropriate parameter values for each test area. Therefore, different combinations of parameters for each filtering algorithm were empirically tested, and optimal parameters were determined in a two-step procedure. First, qualitative analysis was performed by visual examination between the filtered DTM surface and reference DTM surface. If there were significant errors on the surface, detailed statistical analysis was not performed, and the filtering process was repeated by changing the parameters. For detecting a significant error, a visual examination was utilized between DTM surfaces and shaded relief maps generated by the reference and filtered point clouds. Based on visual examinations, obvious errors could be detected by investigating topographic changes, such as removing or preserving obvious features like mounds or buildings. If there was an apparent difference in the surfaces, the second step of the process was not initiated. However, if there was no significant difference between the filtered and reference surfaces, the second step was carried out.

As indicated above, there are different methods used for creating a reference DTM, such as employing a well-known algorithm (ATIN embedded in Terrasolid) for gathering ground data by field measurement (GNSS, Total Station). However, none of the filtering algorithms performs ideally in all terrain surfaces; moreover, field measurements can only be performed in limited areas, and they are highly time-consuming and costly (Julge et al., 2014). For selecting the correct ground data, we used manual classification based on hand filtering via the detailed examination of satellite photographs, intensity views, and lidar point clouds. The reference DTM was generated using these correct ground data.

In the second step of this study, qualitative and quantitative analyses were conducted for different DTM surfaces (generated by extracting the filtered DTM from the reference DTM). Qualitative analysis was performed via the visual examination of different DTM surfaces. Quantitative assessment was done by

Baris Suleymanoglu, Metin Soycan | PRIMERJAVA ALGORITMOV ZA FILTRIRANJE ZA IZDELAVO DMR IZ LIDARSKIH PODATKOV: ŠTUDIJSKI PRIMER BERGAMA, TURČIJA | COMPARISON OF FILTERING ALGORITHMS USED FOR DTM PRODUCTION FROM AIRBORNE LIDAR DATA: A CASE STUDY IN BERGAMA, TURKEY | 395-414 |

| 402 |

calculating statistical values, such as the minimum, maximum, RMS, mean, and median of different DTM surfaces. RMS is the most important statistical value for determining the parameters of filtering algorithms (Aguilar and Mills 2008; Liu et al., 2015). The RMS value was calculated according to discrepancies between Z values of the reference grid nodes (Z_{ref}) and those at the same locations (x, y) of filtered DTM grid nodes ($Z_{flt-alg}$) in these two surfaces:

$$\Delta Z(x_i, y_i) = Z_{flt-alg}(x_i, y_i) - Z_{ref}(x_i, y_i), \tag{1}$$

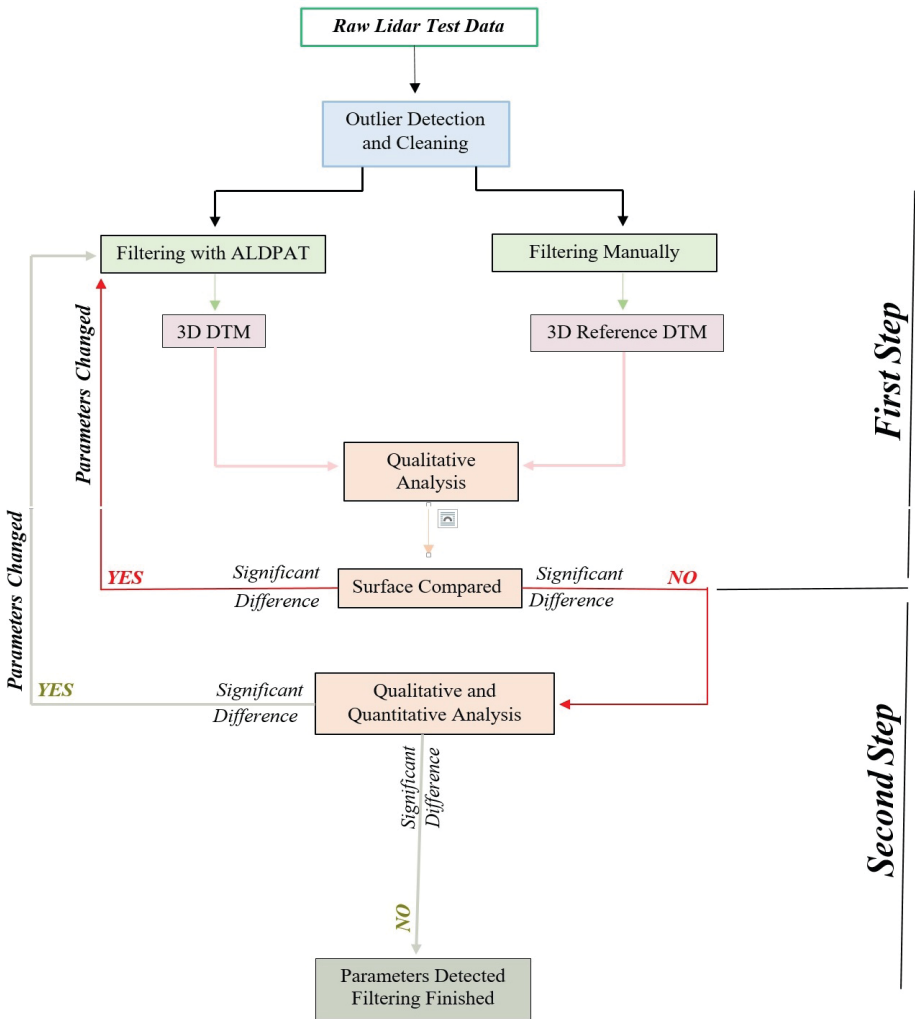$$RMS = \sqrt{\frac{\sum_{i=1}^{n} \Delta Z_i}{n}}, \tag{2}$$

SI | EN

Figure 2: The workflow applied to determine appropriate filtering parameters (Adopted from Sulaiman et al., 2010)

Baris Suleymanoglu, Metin Soycan | PRIMERJAVA ALGORITMOV ZA FILTRIRANJE ZA IZDELAVO DMR IZ LIDARSKIH PODATKOV: ŠTUDIJSKI PRIMER BERGAMA, TURČIJA | COMPARISON OF FILTERING ALGORITHMS USED FOR DTM PRODUCTION FROM AIRBORNE LIDAR DATA: A CASE STUDY IN BERGAMA, TURKEY | 395-414 |

| 403 |

where n is the number of observations and $i = 1, 2, …, n$. RMS values can be affected by gross errors. The error distributions at certain intervals were determined, as shown in Table 4. A significant part of the results consists of the yellow component in the range of –20 to +20 cm, which is the acceptable error range. Positive errors were divided into three different ranges, which were as follows: 0.2 to 0.5 m, 0.5 to 1 m, and >1 m (areas where commission errors occurred). In addition, negative errors were divided into three different ranges, specifically, –0.2 to –0.5 m, –0.5 to –1 m, and <–1 m (areas where omission errors occurred). As a result of all these qualitative and quantitative analyses, the most suitable filtering algorithms for all the test areas and parameter values of this algorithm were determined. The parameter values for each filtering algorithm are shown in Table 2.

Table 2: Determined filtering parameters for all test area (Units are in meters)

Adaptive TIN (ATIN)	Cell Size	Z Difference (m)	Init TriGrid Size (m)	Tile X Width (m)	Tile Y Width (m)	Tile Buffer
First Test Area	0.75	0.3	10	200	200	20
Second Test Area	0.6	0.2	25	200	200	20
Third Test Area	0.5	0.2	10	200	200	20
Fourth Test Area	1	0.8	10	20	20	2

Progressive Morphology (PM)	Cell Size	Window Base(m)	Power Increment	Max. Window Length(m)	Slope(deg)	Initial Threshold(m)
First Test Area	0.75	2	1	8	0.8	0.3
Second Test Area	0.5	2	1	8	0.3	0.2
Third Test Area	0.5	2	1	8	0.3	0.2
Fourth Test Area	1	2	1	8	1	0.4

Maximum Local Slope	Width(m)	Height(m)	Search Radius (m)	Minimum Distance (m)	Maximum Slope(m)
First Test Area	0.75	0.75	5	2	0.8
Second Test Area	0.6	0.6	20	1	0.5
Third Test Area	0.5	0.5	10	2	0.3
Fourth Test Area	2	2	1	1	0.3

Elevation Threshold with Expanding Window (ETEW)	Width(m)	Height(m)	Slope (deg)	Loop Times	Multiscale Curvature Classification (MCC)	Scale	Curvature Threshold
First Test Area	0.75	0.75	0.5	1		2.5	0.3
Second Test Area	0.5	0.5	0.3	7		3	0.3
Third Test Area	0.75	0.75	0.5	1		2	0.3
Fourth Test Area	1	1	0.3	1		1.5	0.3

Iterative Polynomial Fitting (IPF)	Cell Size	Z Difference	Outlier Tolerance	Init Window Length
First Test Area	1.5	0.8	0.1	3
Second Test Area	1.5	1	0.5	20
Third Test Area	2	0.3	0.3	20
Fourth Test Area	2	0.2	0.3	20

Baris Suleymanoglu, Metin Soycan | PRIMERJAVA ALGORITMOV ZA FILTRIRANJE ZA IZDELAVO DMR IZ LIDARSKIH PODATKOV: ŠTUDIJSKI PRIMER BERGAMA, TURČIJA | COMPARISON OF FILTERING ALGORITHMS USED FOR DTM PRODUCTION FROM AIRBORNE LIDAR DATA: A CASE STUDY IN BERGAMA, TURKEY | 395-414 |

| 404 |

4 ANALYSIS OF COMPARISON RESULTS

Filtering was performed for all four test areas using six different filtering algorithms with specified parameters, as shown in Table 2. The test studies indicated that all the filtering algorithms generated commission errors (incorrectly classifying nonground points as ground points) or omission errors (ground points mistakenly classified as nonground points) at different levels. The ΔZ value of the different DTM surfaces between the filtered DTM and reference DTM are shown in Figures 3 and 4. These ΔZ values were separated into seven different ranges. Each range was labelled in a different colour (positive values indicate commission errors and negative values indicate omission errors), and the distributions of these errors were visually examined. The statistical values of the different DTM surfaces are listed in Table 3. The error distributions are shown in Table 4.

Table 3: The statistical values calculated for all test area (Units are in meters)

	Statistical Measures	ATIN-Ref	MLS-Ref	ETEW-Ref	PM-Ref	MCC-Ref	IPF-Ref
First Test Area	Max	3.47	1.77	12.2	3.25	7.9	2.33
	Min	-5	-3.2	-5.42	-3.54	-4.39	-4.37
	RMS	**0.17**	**0.17**	**0.17**	**0.16**	**0.21**	**0.14**
	Mean	0.045	0.048	0.018	0.04	0.087	0.03
	Median	0.017	0.018	0.004	0.016	0.048	0.017
Second Test Area	Max	14.11	9.40	8.68	7.04	18.23	5.36
	Min	-5.63	-5.98	-5.98	-5.68	-6.29	-5.97
	RMS	**0.51**	**0.57**	**0.55**	**0.47**	**0.86**	**0.33**
	Mean	0.11	-0.019	-0.024	0.12	0.1	0.054
	Median	0.013	0.002	0.004	0.017	0.014	0.025
Third Test Area	Max	0.52	0.57	0.56	0.52	1.45	0.40
	Min	-0.48	-0.48	-0.54	-0.48	-0.46	-0.55
	RMS	**0.077**	**0.079**	**0.083**	**0.075**	**0.088**	**0.074**
	Mean	-0.016	-0.01	-0.042	-0.018	0.02	0.01
	Median	-0.019	-0.01	-0.043	-0.02	0.013	0.008
Fourth Test Area	Max	3.65	9.41	7.37	2.98	3.24	2.86
	Min	-8.00	-12.47	-10.51	-7.75	-8.92	-15
	RMS	**0.22**	**0.27**	**0.17**	**0.18**	**0.18**	**0.25**
	Mean	0	-0.06	-0.04	-0.029	0.03	-0.004
	Median	-0.03	-0.07	-0.047	-0.04	0.015	-0.002

Since the first test area was composed of complex surfaces (hills, low and high vegetation, flat areas), multiple commission errors were observed to occur in the regions with sudden elevation or slope changes. Several tree measurements in a vegetation area were not removed, and commission errors occurred at different rates. The minimum and maximum error values differed for each filtering algorithm in the first test area. Therefore, the mean value was found to be different for each algorithm. However, it was seen that similar RMS values were obtained with all the filtering algorithms except MCC.

The ETEW filtering algorithm generally produced commission errors in regions where sudden slope and elevation changes occurred. Several tree objects in hilly areas were not removed, leading to small bumps in the shaded relief DTM, as shown in Figure 3b. The ETEW filtering algorithm generated omission errors on discontinuous surfaces, such as steep slopes (Figure 3b). An RMS value of 17 cm was obtained with the ETEW filtering algorithm, as shown in Table 3. The ATIN algorithm produced commission errors similar to those of the other algorithms. As shown in Figure 3a, it produced errors where elevation differences occurred, such as in passages along rural roads to vegetation areas, vegetation in hilly areas, and trees located on the open landscape. Moreover, such low vegetation was found to generate erroneous results when filtering low objects near the ground. Thus, the threshold value was insufficient to filter such objects.

With the PM filtering algorithm, similar results were obtained to those of ATIN, as shown in Figure 3d. Omission and commission errors were produced in almost the same areas. The best result for the first test area was obtained using the IPF algorithm. An RMS error of 14 cm was obtained with IPF, and 89.9% of the errors were in the range of –20 to +20 cm, as illustrated in Tables 3 and 4; however, the IPF filtering algorithm produced the most omission errors. The omission errors generated by the MLS filtering algorithms occurred on discontinuous surfaces and sunken areas on the ground, as shown in Figure 3c. Like for the other filtering algorithms, commission errors were generated in areas where height and slope changes were experienced. The maximum commission error was generated with the MCC filtering algorithm. Commission errors were produced in nearly all the vegetation-covered hilly mountain areas where elevation changes were experienced.

The second test area consisted of dense settlement areas, large irregularly shaped buildings, and small hilly areas. The small hilly area located at the bottom right of our study area was preserved by all the filtering algorithms. In contrast, the algorithms all produced omission and commission errors at different rates in dense residential areas. As shown in Table 3, the maximum and minimum error values increased for each filtering algorithm. The error values at –20 to +20 cm were much lower than they were in other test areas, as illustrated in Table 4. Therefore, the highest RMS value for all the filtering algorithms was obtained in the second study area.

The best filtering algorithms in the area where the complex buildings were located were ATIN and IPF. The PM algorithm preserved the small mounds in the upper left and lower right corners of the second test area. ATIN, ETEW, MCC, MLS, and PM produced few omission errors in the upper left corner. Moreover, ETEW, PM, MCC, and MLS did not fully filter complex buildings, and thus, they produced commission errors. In the lower-left and upper right corners of the test area, in the region where the elevation suddenly changed, the ground surface was removed by the IPF algorithm and surface abrasion was generated in the shaded relief, as shown in Figure 3l. Such problems can be caused by a border effect. To avoid this, filtering can be applied to an area that is larger than the test area, and then the image can be cropped to the test area to show the results.

ETEW could not fully filter complex buildings, leading to commission errors. The ETEW filtering algorithm removed the terrain point that caused omission errors throughout the settlement area. This led to distortions in the DTM, as shown in Figure 3(h,h). The highest omission error was obtained by the ETEW filtering algorithm, as shown in Table 4. An RMS value of 57 cm was obtained using the

Baris Suleymanoglu, Metin Soycan | PRIMERJAVA ALGORITMOV ZA FILTRIRANJE ZA IZDELAVO DMR IZ LIDARSKIH PODATKOV: ŠTUDIJSKI PRIMER BERGAMA, TURČIJA | COMPARISON OF FILTERING ALGORITHMS USED FOR DTM PRODUCTION FROM AIRBORNE LIDAR DATA: A CASE STUDY IN BERGAMA, TURKEY | 395-414 |

| 406 |

MLS filtering algorithm, which produced high omission errors in dense residential areas, like the ETEW filtering algorithm. In addition, complex structures could not be filtered by the MLS algorithm, as shown in Figure 3 (k,k). The best result for the second test area was obtained by the IPF algorithm with an RMS value of 33 cm, as illustrated in Table 3; however, this algorithm caused erosion in the lower left and upper right corners of the work area. According to the statistical findings, the worst result for the second test area was obtained by the MCC filtering algorithm; here, an RMS error value of 86 cm was calculated, as shown in Table 3. Complex structures could not be filtered with this algorithm, causing intense commission errors in those regions.
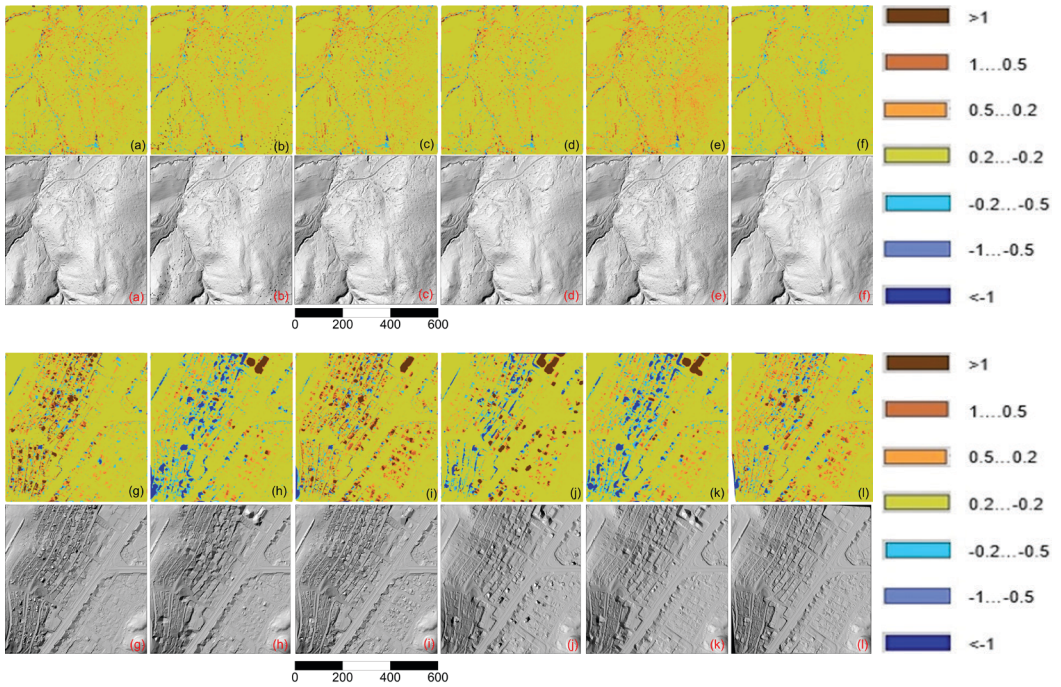

Figure 3: Difference DTM for first test area: a) ATIN-Ref, b) ETEW-Ref, c) MLS-Ref, d) PM-Ref e) MCC-Ref f) IPF-Ref Shaded Relief Map for first test area: a) ATIN, b) ETEW, c) MLS, d) PM, e) MCC, f) IPF Difference DTM for second test area: g) ATIN-Ref, h) ETEW-Ref, i) PM-Ref, j) MCC-Ref, k) MLS-Ref, l) IPF-Ref Shaded Relief Map for second test area: g) ATIN, h) ETEW, i) PM, j) MCC, k) MLS, l) IPF

The lowest RMS values were observed in the third test area. All the filtering algorithms produced values of 7–8 cm, as shown in Table 3. In addition, it was found that the maximum and minimum error values were extremely low compared with those in the other test areas. Accordingly, the mean and median values were found to be close to each other. In Figure 4, it can be seen that almost all the filtering algorithms successfully filtered shrubs and crops. The error values in the –20 to +20 cm range were over 95% for all the filtering algorithms. Based on these results, all the algorithms can filter low vegetation on nearly flat surfaces.

The fourth test area was selected from a valley covered with dense vegetation, with riverbeds, transmission lines, and areas of mixed low and high trees. As shown in Table 4, the omission errors of all the filtering algorithms increased dramatically. Significant omission and commission errors were concentrated along
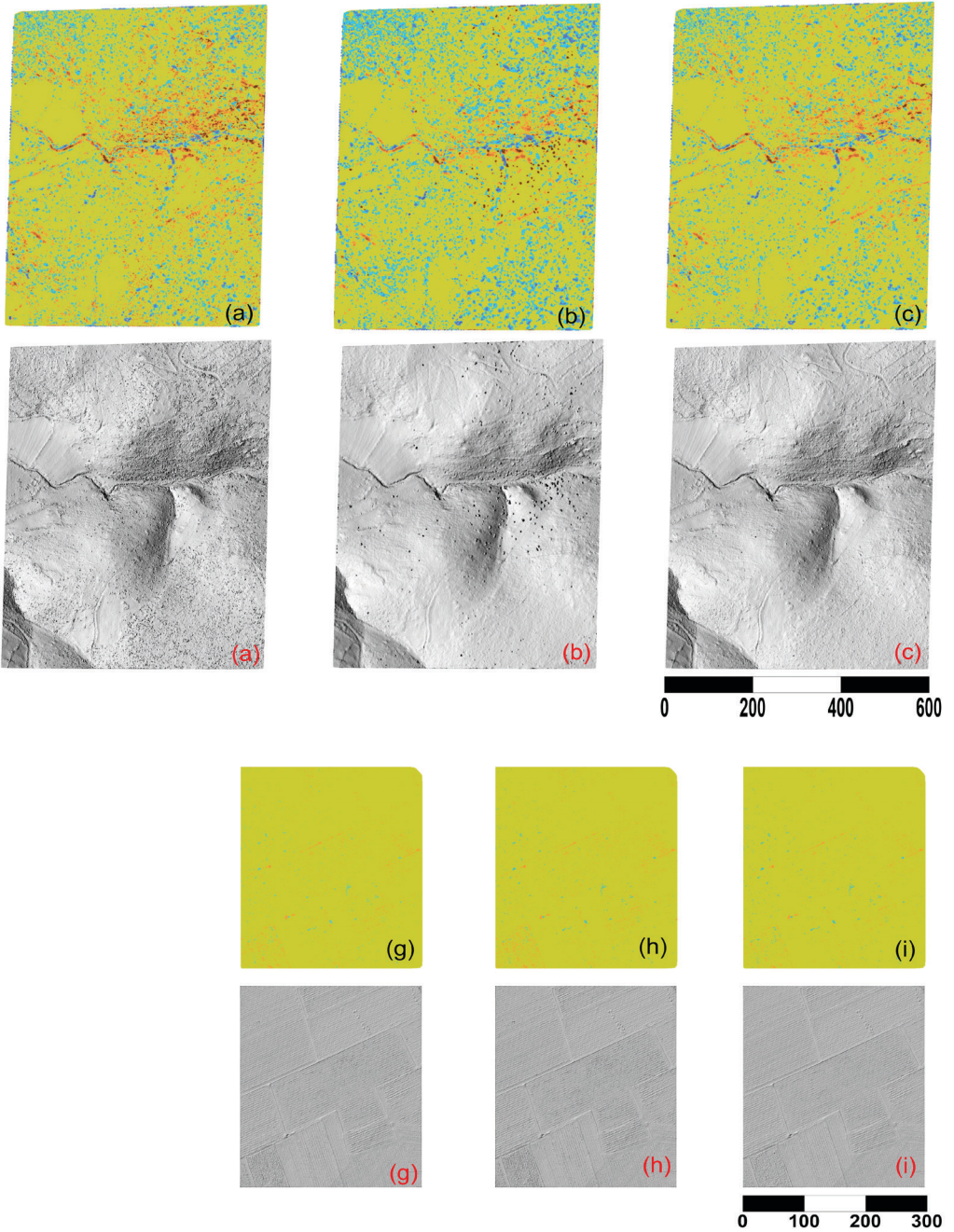
Baris Suleymanoglu, Metin Soycan | PRIMERJAVA ALGORITMOV ZA FILTRIRANJE ZA IZDELAVO DMR IZ LIDARSKIH PODATKOV: ŠTUDIJSKI PRIMER BERGAMA, TURČIJA | COMPARISON OF FILTERING ALGORITHMS USED FOR DTM PRODUCTION FROM AIRBORNE LIDAR DATA: A CASE STUDY IN BERGAMA, TURKEY | 395-414 |

| 407 |

SI | EN

Figure 4: Difference DTM for fourth test area: a) ATIN-Ref, b) MLS-Ref, c) PM-Ref, d) MCC-Ref e) ETEW-Ref f) IPF Shaded Relief Map for fourth test area: a) ATIN, b) MLS, c) PM, d) MCC, e) ETEW, f) IPF Difference DTM for third test area: g)
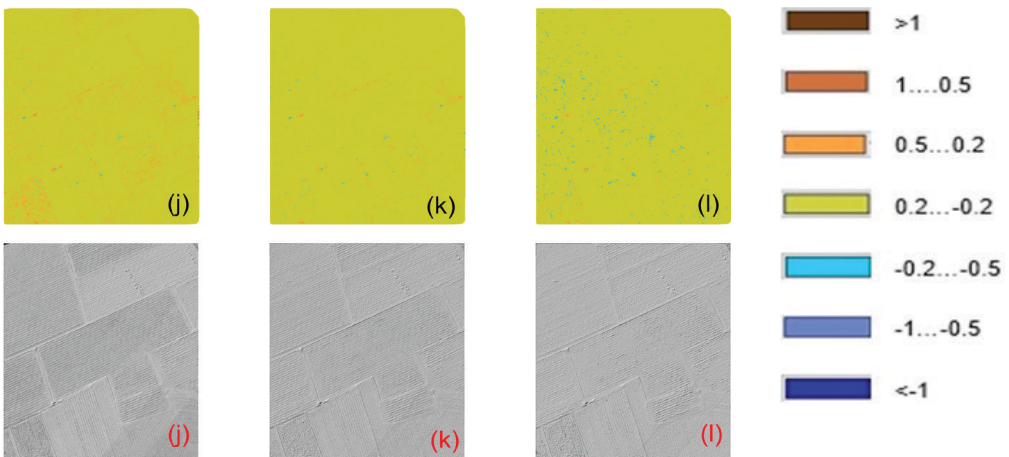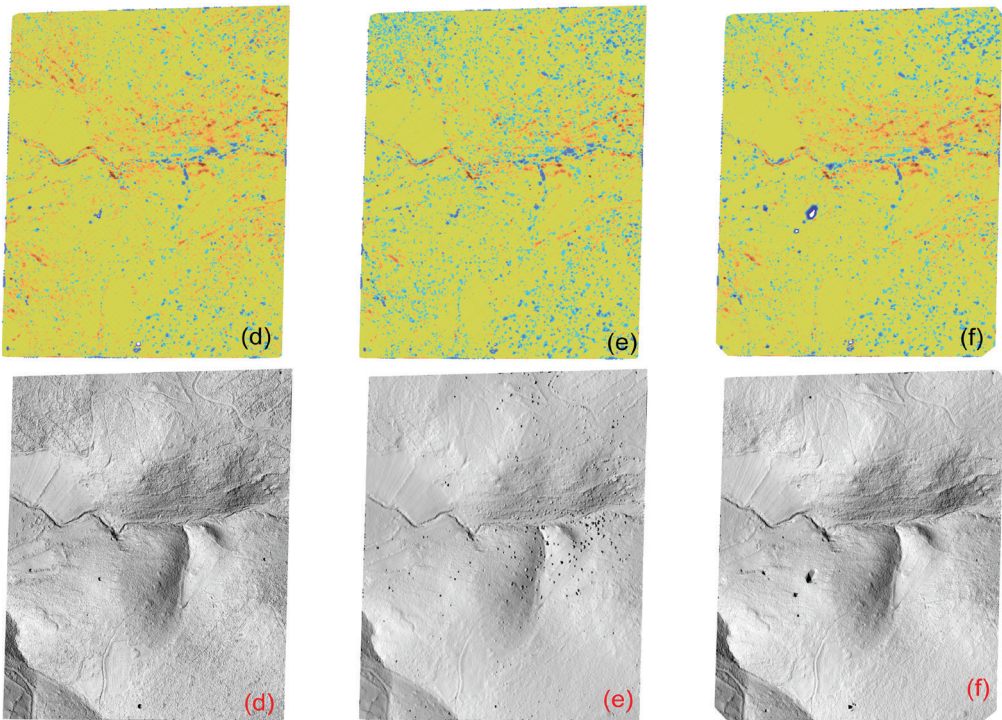
ATIN-Ref, h) MLS-Ref, i) PM-Ref, j) MCC-Ref, k) IPF-Ref, l) ETEW-Ref Shaded Relief Map for third test area: g) ATIN, h) MLS, i) PM, j) MCC, k) IPF, l) ETEW

Baris Suleymanoglu, Metin Soycan | PRIMERJAVA ALGORITMOV ZA FILTRIRANJE ZA IZDELAVO DMR IZ LIDARSKIH PODATKOV: ŠTUDIJSKI PRIMER BERGAMA, TURČIJA | COMPARISON OF FILTERING ALGORITHMS USED FOR DTM PRODUCTION FROM AIRBORNE LIDAR DATA: A CASE STUDY IN BERGAMA, TURKEY | 395-414 |

| 409 |

the riverbeds and valley ridges, as shown in Figure 4a–f. The height difference is one of the basic elements used to separate ground and nonground objects. Since vegetation was located on a sloping surface in our fourth test area, the filtering algorithms were not effective in separating bare earth and vegetation, and they caused omission errors (Sithole and Vosselman, 2004). Since the omission errors were high, it can be the conclusion that the minimum error value had the highest value for all the algorithms.

Table 4: Percentage of error rates for all test area

	Total Commission Error (%)				Total Omission Error (%)				±20cm (%)			
	First	Second	Third	Fourth	First	Second	Third	Fourth	First	Second	Third	Fourth
MLS-Ref	11.6	10.4	1.2	4.7	2.4	12.3	0.4	16.6	86	77.3	98.4	78.8
MCC-Ref	18	16.1	3	11.6	1.9	7.2	0.2	5.5	80.2	76.7	96.8	82.9
ATIN-Ref	10.7	16.2	0.8	11.2	2.3	4.9	0.4	9.5	87	78.9	98.7	79.4
ETEW-Ref	10.4	9.3	0.5	5.2	2.4	12.4	1	11.6	87.2	78.3	98.5	83.3
PM-Ref	9.7	19.9	0.6	7	2.4	5.3	0.5	10.6	87.9	74.8	98.9	82.5
IPF-Ref	7.5	16.8	0.7	7.7	2.6	6.3	0.2	7.9	89.9	76.9	99.1	84.4

According to the RMS values in Table 3 and error values between –20 and +20 cm, as shown in Table 4, the MCC, ETEW, and PM algorithms performed better than the other filtering algorithms did. Two filtering algorithms—ETEW and PM—were able to properly eliminate vegetation, as illustrated in Figure 4 c,c,e,e. However, the MLS and MCC algorithms failed to filter vegetation sufficiently and caused tiny divergences on the shaded relief, as can be seen in Figure 4 b,b,d,d. Compared with other filtering algorithms, the highest commission errors were brought about by the ATIN and MCC filtering algorithms. Although the most appropriate parameter values were selected, these algorithms could not separate low vegetation from the ground. MLS was sensitive to slope changes and had lower accuracy than the other filtering algorithms did in terms of its RMS value of 27 cm in Table 3 and 78.8% value between –20 and +20 cm, as illustrated in Table 4. As shown in Figure 4c,c some nonground data were falsely classified as ground points, which led to small bumps in the shaded relief map. In addition, the highest commission error was obtained by the MLS algorithm, and this was spread over almost the entire test area, although 84.4% of the errors were in the range of –20 and +20 cm, as can be observed in Table 4. An RMS value of 25 cm was obtained by the IPF filtering algorithm, representing the second-worst result. IPF has difficulty filtering local sharp surfaces, and it removed some sharp hilly areas, as illustrated in Figure 4f,f. Furthermore, IPF had edge effects that removed the edges of the test areas.

5 DISCUSSION

The worst result in the first test area among the six filtering algorithms was obtained from MCC, in which the smallest number of correctly filtered points (at –20 to +20 cm) was obtained. All the filtering algorithms except MCC performed well for the first test area. The best result was obtained with IPF, with an RMS of 14 cm. In this test area, commission errors were more common than omission errors were. Commission errors generally occurred in areas where sudden slope and height changes were experienced in the topography and there were natural or artificial objects close to the ground surface. In this context, the determination of the optimal value of the slope or height difference parameters used by the filtering algorithms has a significant effect on reducing errors and improving the results.

Baris Suleymanoglu, Metin Soycan | PRIMERJAVA ALGORITMOV ZA FILTRIRANJE ZA IZDELAVO DMR IZ LIDARSKIH PODATKOV: ŠTUDIJSKI PRIMER BERGAMA, TURČIJA | COMPARISON OF FILTERING ALGORITHMS USED FOR DTM PRODUCTION FROM AIRBORNE LIDAR DATA: A CASE STUDY IN BERGAMA, TURKEY | 395-414 |

| 410 |

As a result of the work done on the second test area, significant increases were seen in omission, commission, and total errors. Accordingly, there was a decrease in the number of points in the range of –20 to +20 cm. Most omission errors were obtained with the MLS, MCC, and ETEW algorithms. In contrast, the least commission errors were obtained by MLS and ETEW. The complex structures were filtered well by the ATIN and IPF algorithms. However, IPF deleted some of the data in the top and bottom corners of the workspace, which corrupted the surface. The best result for the second study area was obtained with the IPF filtering algorithm, with an RMS value of 33 cm.

The best results were found in the third test area. All the filtering algorithms successfully filtered low vegetation. The maximum number of correctly filtered points (at –20 to +20 cm) and minimum RMS values were achieved by all the filtering algorithms for the third test area. Thus, the filtering algorithms can filter low vegetation in areas where the slope change is low.

The worst result in the fourth test area among the six filtering algorithms was obtained from MLS, which obtained the lowest number of correctly filtered points (at –20 to +20 cm). MCC, ETEW, and PM performed better than the other filtering algorithms did based on the RMS and number of points in the range of –20 to +20 cm. Significant proportions of omission and commission errors were concentrated along the riverbeds and valley ridges.

As a result of the filtering process in the four different test areas, it is clear that many parameters can affect the filtering accuracy. First, the filtering performance changes depending on the terrain topography and environmental conditions. Second, the correct selection of the filtering parameters of each algorithm is important for the accuracy and performance of the filtering results. The parameter values of the filtering algorithms, such as the slope, height threshold value, search ellipses, and initial window size, must be best defined to efficiently filter the work areas that have different characteristic features.

Different studies comparing the similar filtering algorithms to those used in this research have been published. There are some similarities and differences between the results. Although Julge et al. (2014) used the same filtering algorithms, the average RMS in their results was higher than ours. This may be due to the size of the work area or lower point density. Sulaiman et al. (2010) compared the filtering algorithms in only one test field, which was similar to our first test area. ATIN, ETEW, IPF, and MLS performed comparably in the two studies. However, the PM algorithm gave the worst results, unlike in our findings. In another work, Podobnikar and Vrečko (2012) conducted trials in two different test areas. The results showed significant similarities to those obtained from our study. Examining these findings more closely, it can be seen that the filtering algorithms have some common points about their performance and some differences. It is thought that the results may have been affected by the size and complexity of the test areas, point density, and parameter values of the filtering algorithms. To elucidate this possibility, more trial and test studies should be performed.

As a result of the test work done, a single filtering algorithm does not seem to be successful on any land surface. To improve the success of filtering algorithms in different study areas, it is necessary to develop integrated algorithms in which algorithms with different characteristics are used together (Chen et al., 2017). In future research, advanced ground-filtering methods can be developed with a combination of different filtering strategies. In addition, the integration of lidar data and other data sources, such as

Baris Suleymanoglu, Metin Soycan | PRIMERJAVA ALGORITMOV ZA FILTRIRANJE ZA IZDELAVO DMR IZ LIDARSKIH PODATKOV: ŠTUDIJSKI PRIMER BERGAMA, TURČIJA | COMPARISON OF FILTERING ALGORITHMS USED FOR DTM PRODUCTION FROM AIRBORNE LIDAR DATA: A CASE STUDY IN BERGAMA, TURKEY | 395-414 |

| 411 |

intensity information, aerial photographs, and full-waveform data, can make significant contributions to the further development of the algorithms. As a result, new methods that can handle complicated terrain situations can be created.

Conflicts of Interest: The authors declare no conflict of interest.

Literature and references:

Aguilar, F. J., Mills, J. P. (2008). Accuracy assessment of lidar-derived digital elevation models. Photogrammetric Record, 23, 148–169. DOI: https://doi.org/10.1111/j.1477-9730.2008.00476.x

Axelsson, P. (1999). Processing of laser scanner data—algorithms and applications. ISPRS Journal of Photogrammetry and Remote Sensing, 54, 138–147. DOI: https://doi.org/10.1016/S0924-2716(99)00008-8

Axelsson, P. (2000). DEM generation from laser scanner data using adaptive TIN models. International Archives of Photogrammetry and Remote Sensing, 33, 111–118.

Bartels, M., Wei, H. (2010). Threshold-free object and ground point separation in LIDAR data. Pattern Recognition Letters, 31, 1089–1099. DOI: https://doi.org/10.1016/j.patrec.2010.03.007

Briese, C. (2010). Extraction of digital terrain models. Airborne and terrestrial laser scanning, (pp. 135–167). Whittles Publishing, Scotland.

Chen, H. F., Cheng, M., Li, J., Liu, Y. S. (2012). An iterative terrain recovery approach to automated dtm generation from airborne lidar point clouds. In M. Shortis, M., M. Madden (eds.), Xxii Isprs Congress, Technical Commission Iv. DOI: https://doi.org/10.5194/isprsarchives-XXXIX-B4-363-2012

Chen, Q., Wang, H., Zhang, H. C., Sun, M. W. & Liu, X. G. (2016). A Point Cloud Filtering Approach to Generating DTMs for Steep Mountainous Areas and Adjacent Residential Areas. Remote Sensing, 8. DOI: https://doi.org/10.3390/rs8010071

Chen, Z., Gao, B., Devereux, B. (2017). State-of-the-art: DTM generation using airborne LIDAR data. Sensors, 17, 150. DOI: https://doi.org/10.3390/s17010150

Elmqvist, M. (2001). Ground estimation of laser radar data using active shape models. In OEEPE workshop on airborne laserscanning and interferometric SAR for detailed digital elevation models (pp. 1–3).

Evans, J. S., Hudak, A. T. (2007). A multiscale curvature algorithm for classifying discrete return LiDAR in forested environments. IEEE Transactions on Geoscience and Remote Sensing, 45, 1029–1038. DOI: https://doi.org/10.1109/TGRS.2006.890412

Guan, H. Y., Li, J., Yu, Y. T., Zhong, L., Ji, Z. (2014). DEM generation from lidar data in wooded mountain areas by cross-section-plane analysis. International Journal of Remote Sensing, 35, 927–948. DOI: https://doi.org/10.1080/01431161.2013.873833

Habib, A., Ghanma, M., Morgan, M., Al-ruzouq, R. (2005). Photogrammetric and LiDAR data registration using linear features. Photogrammetric Engineering & Remote Sensing, 71, 699–707. DOI: https://doi.org/10.14358/PERS.71.6.699

Haralick, R. M., Shapiro, L. G. (1992). Computer and robot vision, Addison-wesley. Boston&USA

Hodgson, M. E., Jensen, J., Raber, G., Tullis, J., Davis, B. A., Thompson, G., Schuckman, K. (2005). An evaluation of lidar-derived elevation and terrain slope in leaf-off conditions. Photogrammetric Engineering & Remote Sensing, 71, 817–823. DOI: https://doi.org/10.14358/PERS.71.7.817

Hu, X. Y., Yuan, Y. (2016). Deep-Learning-Based Classification for DTM Extraction from ALS Point Cloud. Remote Sensing, 8. DOI: https://doi.org/10.3390/rs8090730

Jahromi, A. B., Zoej, M. J. V., Mohammadzadeh, A., Sadeghian, S. (2011). A Novel Filtering Algorithm for Bare-Earth Extraction From Airborne Laser Scanning Data Using an Artificial Neural Network. Ieee Journal of Selected Topics in Applied Earth Observations and Remote Sensing, 4, 836–843. DOI: https://doi.org/10.1109/JSTARS.2011.2132793

Jutzi, B., Stilla, U. (2005). Waveform processing of laser pulses for reconstruction of surfaces in urban areas. Measurement Techniques, 2 (3.1), 2.

Julge, K., Ellmann, A., Gruno, A. (2014). Performance analysis of freeware filtering algorithms for determining ground surface from airborne laser scanning data. Journal of Applied Remote Sensing, 8, 083573. DOI: https://doi.org/10.1117/1.JRS.8.083573

Kayi, A., Erdoğan, M., Eker, O. (2015). OPTECH HA-500 ve RIEGL LMS-Q1560 ile gerçekleştirilen LİDAR test sonuçları. Harita dergisi, 153, 42–46.

Khosravipour, A., Skidmore, A. K., Isenburg, M., Wang, T. J., Hussin, Y. A. (2014). Generating Pit-free Canopy Height Models from Airborne Lidar. Photogrammetric Engineering and Remote Sensing, 80, 863–872.

Kilian, J., Haala, N., Englich, M. (1996). Capture and evaluation of airborne laser scanner data. International Archives of Photogrammetry and Remote Sensing, 31, 383–388.

Kraus, K., Pfeifer, N. (1998). Determination of terrain models in wooded areas with airborne laser scanner data. ISPRS Journal of Photogrammetry and Remote Sensing, 53, 193–203. DOI: https://doi.org/10.1016/S0924-2716(98)00009-4

Krishnan, S., Crosby, C., Nandigam, V., Phan, M., Cowart, C., Baru, C., Arrowsmith, R.(2011). OpenTopography: a services oriented architecture for community access to LIDAR topography. Proceedings of the 2nd International Conference on Computing for Geospatial Research & Applications. ACM, 7. DOI: https://doi.org/10.1145/1999320.1999327

Li, Y., Yong, B., Wu, H., An, R., Xu, H. (2014). An improved top-hat filter with sloped brim for extracting ground points from airborne lidar point clouds. Remote Sensing, 6, 12885–12908. DOI: https://doi.org/10.3390/rs61212885

Baris Suleymanoglu, Metin Soycan | PRIMERJAVA ALGORITMOV ZA FILTRIRANJE ZA IZDELAVO DMR IZ LIDARSKIH PODATKOV: ŠTUDIJSKI PRIMER BERGAMA, TURČIJA | COMPARISON OF FILTERING ALGORITHMS USED FOR DTM PRODUCTION FROM AIRBORNE LIDAR DATA: A CASE STUDY IN BERGAMA, TURKEY |395-414|

| 412 |

Liu, X. (2008). Airborne LiDAR for DEM generation: some critical issues. Progress in Physical Geography, 32, 31–49. DOI: https://doi.org/10.1177/0309133308089496

Liu, X. H., Hu, H., Hu, P. (2015). Accuracy Assessment of LiDAR-Derived Digital Elevation Models Based on Approximation Theory. Remote Sensing, 7, 7062–7079. DOI: https://doi.org/10.3390/rs70607062

Mallet, C., Bretar, F., Roux, M., Soergel, U., Heipke, C. (2011). Relevance assessment of full-waveform lidar data for urban area classification. Isprs Journal of Photogrammetry and Remote Sensing, 66, S71–S84. DOI: https://doi.org/10.1016/j.isprsjprs.2011.09.008

Mongus, D., Cekada, M. T., Zalik, B. (2013). The analysis of an automatic method for digital terrain model generation from lidar data on slovenian test cases. Geodetski vestnik, 57, 245–259.

Mongus, D., Lukač, N., Žalik, B. 2014. Ground and building extraction from LiDAR data based on differential morphological profiles and locally fitted surfaces. ISPRS Journal of Photogrammetry and Remote Sensing, 93, 145–156. DOI: https://doi.org/10.1016/j.isprsjprs.2013.12.002

Pfeifer, N., Mandlburger, G. 2018. 11 LiDAR Data Filtering and Digital Terrain Model Generation. Topographic Laser Ranging and Scanning: Principles and Processing, 349. Taylor &Francis, London

Pfeifer, N., Stadler, P., Briese, C. 2001. Derivation of digital terrain models in the SCOP++ environment. Proceedings of OEEPE Workshop on Airborne Laserscanning and Interferometric SAR for Detailed Digital Terrain Models, Stockholm, Sweden.

Pingel, T. J., Clarke, K. C., Mcbride, W. A. (2013). An improved simple morphological filter for the terrain classification of airborne LIDAR data. ISPRS Journal of Photogrammetry and Remote Sensing, 77, 21–30. DOI: https://doi.org/10.1016/j.isprsjprs.2012.12.002

Podobnikar, T., Vrečko, A. (2012). Digital elevation model from the best results of different filtering of a LiDAR point cloud. Transactions in GIS, 16, 603–617. DOI: https://doi.org/10.1111/j.1467-9671.2012.01335.x

Silva, C. A., Klauberg, C., Hentz, Â. M. K., Corte, A. P. D., Ribeiro, U., Liesenberg, V. (2018). Comparing the performance of ground filtering algorithms for terrain modeling in a forest environment using airborne LiDAR data. Floresta e Ambiente, 25 (2). DOI: https://doi.org/10.1590/2179-8087.015016

Sithole, G., Vosselman, G. (2001). Filtering of laser altimetry data using a slope adaptive filter. International Archives of Photogrammetry Remote Sensing and Spatial Information Sciences, 34, 203–210.

Sithole, G., Vosselman, G. (2004). Experimental comparison of filter algorithms for bare-Earth extraction from airborne laser scanning point clouds. ISPRS journal of photogrammetry and remote sensing, 59, 85–101. DOI: https://doi.org/10.1016/j.isprsjprs.2004.05.004

Sithole, G., Vosselman, G. (2005). Filtering of airborne laser scanner data based on segmented point clouds. International Archives of Photogrammetry, Remote Sensing and Spatial Information Sciences, 36, W19.

Sohn, G.; Dowman, I. J. (2002). Terrain surface reconstruction by the use of tetrahedron model with the MDL criterion. In: International Archives of Photogrammetry Remote Sensing and Spatial Information Sciences. NATURAL RESOURCES CANADA, p. 336–344.

Sulaiman, N. S., Majid, Z., Setan, H. (2010). DTM generation from LiDAR data by using different filters in open-source software. Geoinformation Science Journal, 10 (2), 89–109.

Susaki, J. (2012). Adaptive slope filtering of airborne LiDAR data in urban areas for digital terrain model (DTM) generation. Remote Sensing, 4, 1804–1819. DOI: https://doi.org/10.3390/rs4061804

Tóvári, D., Pfeifer, N. (2005). Segmentation based robust interpolation-a new approach to laser data filtering. International Archives of Photogrammetry, Remote Sensing and Spatial Information Sciences, 36, 79–84.

Vosselman, G. (2000). Slope based filtering of laser altimetry data. International Archives of Photogrammetry and Remote Sensing, 33, 935–942.

Vosselman, G., Oude Elberink, S., Post, M., Stoter, J., Xiong, B., Frietsch, D. (2015). From nationwide point clouds to nationwide 3D landscape models. Photogrammetric Week'15.

Wehr, A., Lohr, U. (1999). Airborne laser scanning—an introduction and overview. ISPRS Journal of photogrammetry and remote sensing, 54, 68–82. DOI: https://doi.org/10.1016/S0924-2716(99)00011-8

Wever, C., Lindenberger, J. (1999). Experiences of 10 years laser scanning. In: Photogrammetric Week 99, 1999. Citeseer.

Wu, J., & Liu, L. (2011). Automatic DEM generation from aerial lidar data using multiscale support vector machines. In MIPPR 2011: Remote Sensing Image Processing, Geographic Information Systems, and Other Applications (Vol. 8006, p. 800609). International Society for Optics and Photonics.

Zakšek, K., Pfeifer, N., Iapš, Z. (2006). An improved morphological filter for selecting relief points from a LIDAR point cloud in steep areas with dense vegetation. Institute of Anthropological and Spatial Studies, Scientific Research Centre of the Slovenian Academy of Sciences and Arts: Ljubljana, Slovenia.

Zhang, J. X., Lin, X. G. (2013). Filtering airborne LiDAR data by embedding smoothness-constrained segmentation in progressive TIN densification. ISPRS Journal of Photogrammetry and Remote Sensing, 81, 44–59. DOI: https://doi.org/10.1016/j.isprsjprs.2013.04.001

Zhang, K., Chen, S.-C., Whitman, D., Shyu, M.-L., Yan, J., Zhang, C. (2003). A progressive morphological filter for removing nonground measurements from airborne LIDAR data. IEEE transactions on geoscience and remote sensing, 41, 872–882. DOI: https://doi.org/10.1109/TGRS.2003.810682

Zhang, K., Whitman, D. (2005). Comparison of three algorithms for filtering airborne lidar data. Photogrammetric Engineering & Remote Sensing, 71, 313–324. DOI: https://doi.org/10.14358/PERS.71.3.313

Zhang, K., & Cui, Z. (2007). Airborne LiDAR Data Processing and Analysis Tools—ALDPAT 1.0 Software Manual. Miami, Florida: International Hurricane Research Centre, Department of Environmental Studies, Florida International University, 81p.

Zhang, W. M., Qi, J. B., Wan, P., Wang, H. T., Xie, D. H., Wang, X. Y., Yan, G. J. (2016). An Easy-to-Use Airborne LiDAR Data Filtering Method Based on Cloth Simulation. Remote Sensing, 8. DOI: https://doi.org/10.3390/rs8060501

Zhao, X. Q., Su, Y. J., Li, W. K., Hu, T. Y., Liu, J., Guo, Q. H. (2018). A Comparison of LiDAR Filtering Algorithms in Vegetated Mountain Areas. Canadian Journal of Remote Sensing, 44, 287–298. DOI: https://doi.org/10.1080/07038992.2018.1481738

Baris Suleymanoglu, Metin Soycan | PRIMERJAVA ALGORITMOV ZA FILTRIRANJE ZA IZDELAVO DMR IZ LIDARSKIH PODATKOV: ŠTUDIJSKI PRIMER BERGAMA, TURČIJA | COMPARISON OF FILTERING ALGORITHMS USED FOR DTM PRODUCTION FROM AIRBORNE LIDAR DATA: A CASE STUDY IN BERGAMA, TURKEY | 395-414 |

| 413 |

Baris Suleymanoglu, M.Sc.
Yildiz Technical University Civil Engineering, Faculty Department of Geomatic Engineering
Davutpasa street 34220 – Esenler – Istanbul, Turkey
e-mail: bariss@yildiz.edu.tr

Metin Soycan, PhD - Prof. Dr.
Yildiz Technical University Civil Engineering Faculty Department of Geomatic Engineering
Davutpasa street 34220 – Esenler – Istanbul, Turkey
e-mail: soycan@yildiz.edu.tr

Baris Suleymanoglu, Metin Soycan | PRIMERJAVA ALGORITMOV ZA FILTRIRANJE ZA IZDELAVO DMR IZ LIDARSKIH PODATKOV: ŠTUDIJSKI PRIMER BERGAMA, TURČIJA | COMPARISON OF FILTERING ALGORITHMS USED FOR DTM PRODUCTION FROM AIRBORNE LIDAR DATA: A CASE STUDY IN BERGAMA, TURKEY | 395-414 |

| 414 |